

PX028 - Resolving large unit cells by using the correct detector, distance, and beam divergence

Introduction

Large unit cells pose a challenge for any home lab diffractometer equipped with modern, high-flux confocal multilayer optics with a small beam size ($\leq 100 \mu\text{m}$). The larger the unit cell, the closer the reflections are to each other on a diffraction image. To minimize overlap and resolve these reflections as separate peaks, one usually increases the crystal-to-detector distance, but larger distances result in enlarged reflections due to the divergence of the X-ray beam. Therefore, adjustable divergence on the optics is critical. Here, we will show the screening, data collection, and structure solution for a large unit cell sample using a combination of the correct detector, crystal-to-detector distance, and beam divergence.

Experimental overview

Crystals of StmaA.01026.c.B1 (PDB ID 6W80) were provided by Dr. Jan Abendroth of UCB Seattle[†]. Briefly, crystals were grown from a solution of 13 mg/mL protein in an optimization screen around condition G9 of the Morpheus screen (Molecular Dimensions). All crystals were mounted on a Rigaku XtaLAB SynergyCustom (Table 1) and collected at 100 K.

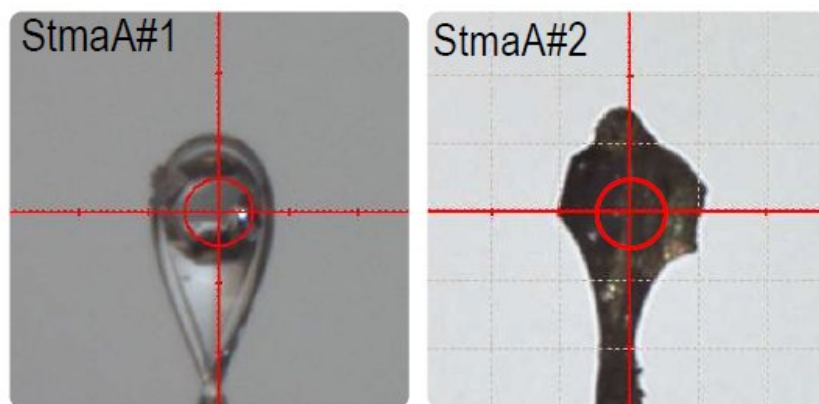


Figure 1: StmaA crystals. Red circle is 0.1 mm in diameter.

Table 1: XtaLAB SynergyCustom specifications

| | |
|----------------------|--|
| X-ray source | FR-X |
| Operating power | 45 kV x 66 mA = 2.97 kW |
| X-ray optic | Confocal VariMax VHF |
| Beam characteristics | FWHM = 100 μm , Divergence = 10 mrad (adjustable) |

| | | |
|-----------------------------|--|--|
| Goniometer / Detector range | 4-circle Kappa with telescoping 2 θ arm / distance range of 31 – 250 mm | |
| Detector | Hybrid photon counting, HyPix-6000HE | Hybrid photon counting, HyPix-Arc 150° |
| Active area | 77.5 x 80.3 mm | 77.5 x 121.8 mm |
| Frame rate | Up to 100 Hz | Up to 70 Hz |
| Pixel size | 100 μ m | 100 μ m |
| Cooling | air-cooled | water-cooled |

[†]The materials described herein were provided by the Seattle Structural Genomics Center for Infectious Disease (www.SSGCID.org), which is supported by Federal Contract No. HHSN272201700059C from the National Institute of Allergy and Infectious Diseases, National Institutes of Health, Department of Health and Human Services.

Results

A crystal of StmaA#1 (125 μ m x 130 μ m x 160 μ m) was mounted on the XtaLAB SynergyCustom with a hybrid photon counting HyPix-6000HE detector (Figure 1). Auto-indexing of crystal screening images revealed a primitive hexagonal cell with dimensions $a=b=60$ Å and $c=367$ Å. When screening images were collected with the full X-ray beam (i.e., divergence of 10 mrad) and a distance of 40 mm, the reflections on the long c -axis were smeary and severely overlapped (Figure 2). Moving the detector to distances of 80, 90, 100, 110, and 120 mm to resolve the long axis reflections helped somewhat, but the effect was offset by the growth in size of the reflections. Therefore, the screening was repeated at the above distances several times with different divergence settings on the optic: 4, 3, 2, and 1.5 mrad.

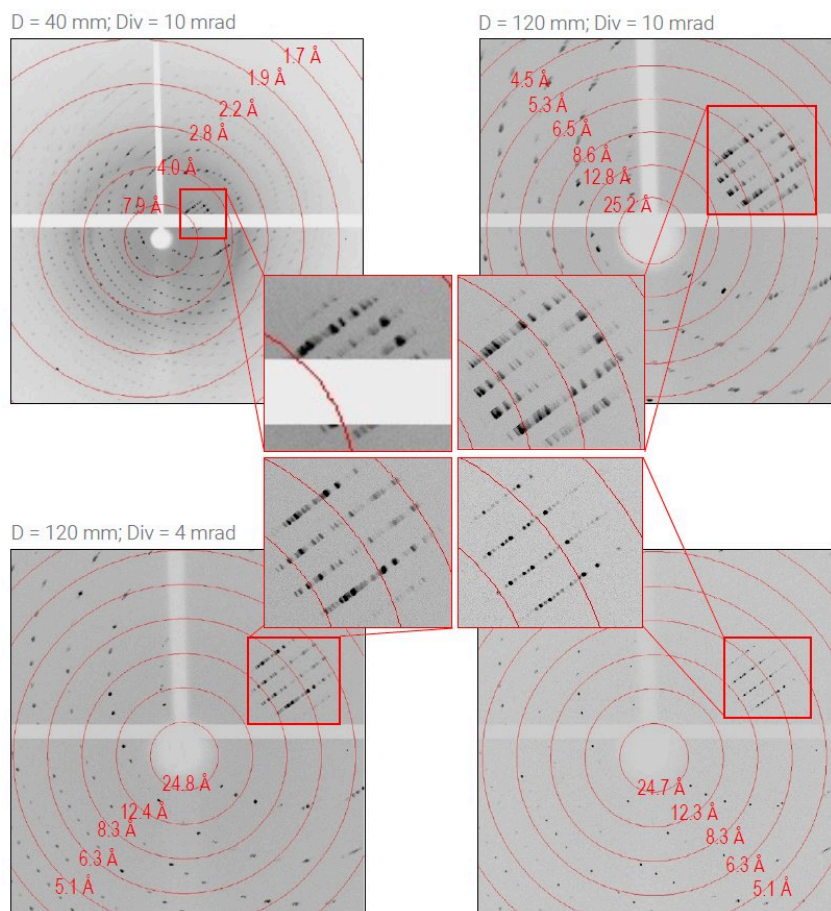


Figure 2: A 5-second exposure per 0.2° rotation of the StmaA#1 crystal on the HyPix-6000HE at the indicated distances and divergence settings. Insets show a zoomed-in view of an area with the same group of reflections that become smaller and better separated with proper distance and divergence.

By examining the images, the separation of reflections on the 367 \AA c-axis appeared the best at a distance of 120 mm and a divergence of 1.5 mrad (Figure 2), but we wanted to apply a more quantitative analysis. First, the percentage of reflections auto-indexed with the correct unit cell was examined. Figure 3 shows that as the crystal-to-detector distance and divergence approached 120 mm and 1.5 mrad, respectively, the most reflections ($>90\%$) were indexed. Next, the separation of the reflections along the 367 \AA c-axis was checked by looking at the distribution of reflections falling on the correct lattice point for c^* (within a standard tolerance). Again, Figure 3 shows that, as the crystal-to-detector distance and divergence approached 120 mm and 1.5 mrad, respectively, the peaks along c^* sharpened. The relationship between this “optimal” distance of 120 mm and c-axis of 367 \AA is factor of ~ 3 .

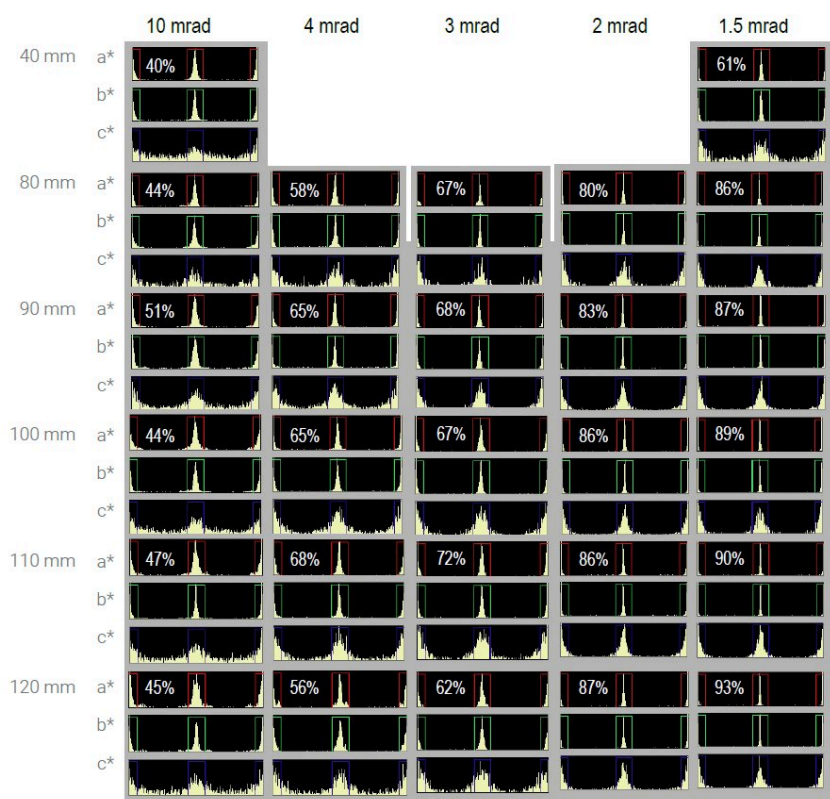


Figure 3: The effect of crystal-to-detector distance and divergence setting on the resolution of a 367 Å c-axis. The distribution histograms of reflections along a*, b*, and c* are shown with the total percentage of auto-indexed reflections indicated.

With the experimental settings optimized, an overnight data collection strategy to collect complete, redundant data to 1.6 Å was calculated and run for StmaA#1 (Table 2). The data were integrated and scaled with CrysAlis^{Pro}, exported to an unmerged mtz file, and merged with AIMLESS¹. The final statistics of mean signal-to-noise and $CC_{1/2}$ supported the high-resolution limit of 1.6 Å (Table 3). The merging R factor of ~10% was quite good. The structure was solved by molecular replacement in Phaser² using PDB entry 6W80 as a search model. Several rounds of model building with Coot³ and restrained refinement with Refmac⁴ produced a final model with reasonable R factors near 20%.

Table 2: Data collection parameters summary

| | StmaA#1 | StmaA#2 |
|----------------------------|-------------|-----------|
| Total # Images | 2368 | 1475 |
| Total # Scans | 8 | 4 |
| Total Data Collection Time | 11h 35m 57s | 2h 3m 40s |

Table 3: Final statistics from data processing and structure solution

| | LY | LY + sucrose |
|-------------|--------------------|--------------------|
| Space group | P6 ₅ 22 | P6 ₅ 22 |

| | | |
|---|-------------------------|-------------------------|
| Unit cell | 60.3 Å, 60.3 Å, 366.7 Å | 60.4 Å, 60.4 Å, 367.3 Å |
| Resolution (last shell) | 25.5–1.6 Å (1.63–1.6 Å) | 26.4–1.6 Å (1.63–1.6 Å) |
| Completeness (last shell) | 99.8% (99.4%) | 99.6% (100%) |
| Redundancy (last shell) | 6.4 (4.1) | 5.8 (4.7) |
| $\langle I/\sigma I \rangle$ (last shell) | 10.4 (1.8) | 12.8 (2.1) |
| R_{merge} (last shell) | 10.7% (68.6%) | 7.6% (65.5%) |
| R_{merge} anomalous (last shell) | 10.1% (62.2%) | 7.1% (57.8%) |
| $CC_{1/2}$ | 1.0 (0.51) | 1.0 (0.58) |
| R_{work} | 22.2% | 19.8% |
| R_{free} | 25.4% | 23.0% |

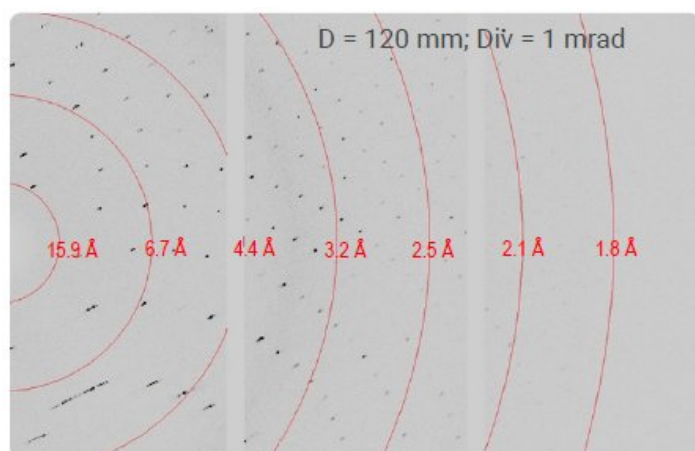


Figure 4: A 5-second exposure per 0.15° rotation of the StmaA#2 crystal on the HyPix-Arc 150° at the indicated distance and divergence settings.

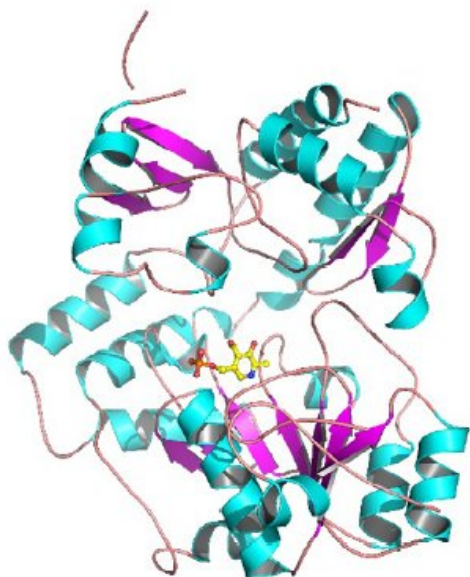


Figure 5: Cartoon showing secondary structure elements of StmaA#2. The helices are cyan and the sheets are purple. A pyridoxal-5'-phosphate is shown in ball and stick representation.

Conclusion

A crystal-to-detector distance of 120 mm and a divergence of 1.5 to 1 mrad was needed to clearly resolve the reflections on a 367 Å c-axis with a HyPix detector and a VariMax VHF optic. Under these experimental settings, high-quality and high-resolution data were collected on two different crystals and HyPix detectors. From this work and observations with other long axis samples with dimensions approaching 500 Å, we recommend using a crystal-to-detector distance of 1/3 the longest primitive cell axis with a HyPix detector and then reducing the divergence to achieve the desired separation of reflections.

References

1. Evans P.R., Murshudov G.N. (2013). *Acta Cryst.* **D69**, 1204-1214.
2. McCoy A.J., et al. (2007). *J Appl Crystallogr.* **40**, 658-674.
3. Emsley P., Lohkamp B., Scott W.G., Cowtan K.(2010). *Acta Cryst.* **D66**, 486-501.
4. Murshudov G.N., et al. (2011). *Acta Cryst.* **D67**, 355-367.

Related products



HyPix-6000HE

Extremely low noise detector based on direct X-ray detection technology.



HyPix-Arc 150°

A curved detector based on direct X-ray detection technology with the highest 2θ range at a single position available for the home lab.



VariMax

Single wavelength Confocal Max-Flux (CMF) optics for single crystal diffraction



XtaLAB SynergyCustom

A bespoke, extremely high-flux diffractometer with custom enclosure and the flexibility to utilize both ports of the rotating anode X-ray source.